Concurrent investigation of global motion and form processing in amblyopia: an equivalent noise approach

Joshi, Mahesh R.; Simmers, Anita J.; Jeon, Seong T.

Published in:
Investigative Ophthalmology and Visual Science

DOI:
10.1167/iovs.15-18609

Publication date:
2016

Document Version
Publisher's PDF, also known as Version of record

Concurrent Investigation of Global Motion and Form Processing in Amblyopia: An Equivalent Noise Approach

Mahesh R. Joshi, Anita J. Simmers, and Seong T. Jeon

Vision Sciences, Department of Life Sciences, Glasgow Caledonian University, Glasgow, United Kingdom

Correspondence: Seong T. Jeon, Vision Sciences, Department of Life Sciences, Glasgow Caledonian University, Glasgow, G4 0BA, United Kingdom;
Simon.Jeon@gcu.ac.uk.

Submitted: November 9, 2015
Accepted: July 19, 2016

Citation: Joshi MR, Simmers AJ, Jeon ST. Concurrent investigation of global motion and form processing in amblyopia: an equivalent noise approach. *Invest Ophthalmol Vis Sci*. 2016;57:5015–5022. DOI:10.1167/iovs.15-18609

Purpose. Directly comparing the motion and form processing in neurologic disorders has remained difficult due to the limitations in the experimental stimulus. In the current study, motion and form processing in amblyopia was characterized using random dot stimuli in different noise levels to parse out the effect of local and global processing on motion and form perception.

Methods. A total of 17 amblyopes (8 anisometropic and 9 strabismic), and 12 visually normal subjects monocularly estimated the global direction of motion and global orientation in random dot kinematograms (RDK) and Glass patterns (Glass), whose directions/orientations were drawn from normal distributions with a range of means and variances that served as external noise. Direction/orientation discrimination thresholds were measured without noise first then variance threshold was measured at the multiples of the direction/orientation threshold. The direction/orientation and variance thresholds were modelled to estimate internal noise and sampling efficiency parameters.

Results. Overall, the thresholds for Glass were higher than RDK for all subjects. The thresholds for both Glass and RDK were higher in the strabismic eyes compared with the fellow and normal eyes. On the other hand, the thresholds for anisometropic amblyopic eyes were similar to the normal eyes. The worse performance of strabismic amblyopes was best explained by relatively low sampling efficiency compared with other groups ($P < 0.05$).

Conclusions. A deficit in global motion and form perception was only evident in strabismic amblyopia. Contrary to the dorsal stream deficiency hypothesis assumed in other developmental disorders, deficits were present in both motion (dorsal) and form (ventral) processing.

Keywords: amblyopia, motion perception, form perception, dorsal stream dysfunction, noise

Amblyopia is a neurodevelopmental disorder characterized by reduction in either monocular or binocular vision without any organic cause. The primary site of the visual deficit in amblyopia is reported to be the striate cortex.[1–3] However, the functional visual deficits in amblyopia seem to spread beyond primary visual cortex to extra striate cortical areas.[4–8]

Global motion direction judgment or perceiving a global orientation from the distribution of locally oriented elements is accomplished in two stages where the local direction and orientation are initially encoded in early visual areas of primary visual cortex/area V2 (V1/V2), after which the global processing is thought to occur at higher extra striate cortical areas; middle temporal area (MT), medial superior temporal (MST) for motion, and V4 for form.[9,10] Behavioral studies in humans have reported reduced sensitivity to both global motion and global form in amblyopia.[11–15] The motion coherence threshold remained elevated even after the local deficits from V1/V2 such as in contrast sensitivity was accounted for.[13,14,16,17] However, other studies have reported normal performance in amblyopes using a different experimental design where the global motion direction judgement was evaluated in varying degrees of local directional noise.[15,18] Global form is also compromised in amblyopes as observed by abnormal global form coherence thresholds for Glass patterns (Glass) and translational/rotational line segments.[12,19,20] However, other studies have reported inconsistent results where discrimination of the mean global orientation from an array of Gabor patches with different orientations is reported to be normal,[15] slightly reduced,[11] or even abnormal.[21]

Several reviews of global motion and form perception in a range of developmental disorders[22–24] including amblyopia[12] indicate that the motion processing is more affected than the form processing. According to the 'two-streams hypothesis',[25] the global motion and form perceptions are processed along the dorsal and ventral streams, respectively, bifurcated from early cortical areas.[26–28] There have been a number of attempts to compare these two domains of vision by measuring the outputs from the processing of the corresponding stream using similar stimuli. For example, studies used translational random dot kinematograms (RDK) for motion and oriented streaks for form created by superimposing the multiple still frames from the respective RDK to compare the amblyopic performance in two streams.[12,29] The results showed deficits along both visual processing streams, with a relatively larger deficit in motion processing (dorsal stream) compared with the form processing (ventral stream). The superimposed orientation streaks are considered, however, no different from line segments where the global integration of local elements does not seem necessary to do the task.[22] It is also difficult to ascertain if the deficit observed in either or both streams is purely stream-

Table 1. The Clinical Details of the Amblyopic Participants

Type of Amblyopia	ID	Age, y	IOD	Refraction		Cover Test	Stereo, arc sec
				RE	LE		
Anisometropic	KW	18	0.1	−6.25/−1.25*170	−6.50/−1.50*180	Exophoria	20
	RK	19	0.22	+1.75/−1.00*180	0.00	Exophoria	85
	LC	18	0.14	+3.75/−1.00*170	+5.25/−1.25*180	Exophoria	36
	HM	18	0.18	−2.75/−3.00*180	−2.25/−1.75*10	Exophoria	75
	MR	20	0.16	+6.00/−3.75*10	+5.00/−3.25*180	Esophoria	100
	LS	19	0.40	+5.25/−0.50*105	+3.50/−0.50*105	Esophoria	No
	MI	19	0.20	−3.50/−0.50*60	−8.50/−1.50*140	Exophoria	40
	HMc	19	0.26	−0.25	+1.00/−1.00*90	Exophoria	20
Strabismic	SS	20	0.41	+4.50/−0.50*172	+5.75/−1.00*22	Esotropia	No
	JR	43	0.48	−2.50	−2.50	Esotropia	No
	CO	20	0.34	+4.00/−1.50*175	+4.50/−1.50*90	Int. Esotropia	200
	HQ	34	0.50	−1.50/−2.00*5	−1.50/−2.00*5	Exotropia	No
	MR	48	0.26	+3.00/−2.50*90	+1.50	Esotropia	No
	SM	28	0.6	+0.50	+3.50/−1.50*90	Exotropia	No
	NJ	21	0.4	+1.00	+3.00	Esotropia	No
	JW	57	0.24	+0.75/−0.25*25	+3.00/−0.50*25	Esotropia	No
	KH	22	0.2	+8.50/−3.50*25	+9.00/−3.00*170	Esotropia	No

IOD, interocular difference; RE, right eye; LE: left eye.

specific, mere collateral damage from the early areas (V1/V2) common to both streams, or a combined effect of both. Direct comparison of the two streams can be made more precise by making stimulus parameters as similar as possible except for the domain specific outputs of interest.

Many psychophysical studies of global processing mechanisms have used coherence tasks where one measures the minimum proportion of coherent elements to random elements needed for a reliable discrimination. However, this paradigm is limited in separating the local influence of the early visual areas (V1/V2) shared by both streams from the global aspect of visual processing by the higher extra striate areas specific to each stream. This limitation can be resolved by measuring outputs in varying levels of noise added to the stimuli.[30]

In the current study, we measured global motion and form discrimination thresholds in normal and amblyopic subjects to probe and compare the differences (or similarities) in their motion and form processing using similar stimulus with and without external noise to investigate how their performance are affected by the local and global parameters of the task.

Methods

Participants

A total of 17 amblyopes (strabismic = 9, anisometropic = 8, mean age = 26.06 ± 12.09 years) with interocular acuity difference (IOD) of greater than or equal to 0.2 logMAR or past history of amblyopia treatment (Table 1), and 12 normal controls (mean age = 28 ± 5.24 years) were recruited. Viewing was monocular in all cases. The control group had normal binocular vision and normal or corrected-to-normal visual acuity. All experiments were conducted with the best (full) correction after refraction by an optometrist, who is one of the authors (MRJ).

The study was conducted in accordance with The Code of Ethics of the World Medical Association, Declaration of Helsinki, and approved by the Life Sciences Human Subjects Research Ethics Committee of the Glasgow Caledonian University. Informed consent was obtained once the nature and possible consequences of the experiment had been explained.

Stimuli

The experimental stimuli were generated using MATLAB 64 bit version R2013a (The MathWorks, Natick, MA, USA) with Psychophysics Toolbox-3 extensions[31,32] and displayed on a 21" Sony FD Trinitron monitor with a pixel resolution of 1920 × 1440 and refresh rate of 75 Hz (Sony, Tokyo, Japan) powered by an Apple computer with OS X (Apple, Cupertino, CA, USA) and ATI Radeon HD 5770 1024 MB graphics card. Across all the experiments, stimulus parameters across domains (i.e., form and motion) were kept identical except for the tasks specific to each domain (orientation versus direction discrimination). For example, both form and motion stimuli were composed of same number of black dots of the same size (0.166°) and contrast (95% Michelson contrast). They were displayed for 0.5 seconds in a circular aperture of 10° when viewed at 50 cm.

For the anisometropes and six normal controls (Experiment 1), both motion and form stimuli were composed of 500 dot elements with a dot density of 12.81 dots/deg^2. The overall dot speed in the motion stimulus (RDK) was 10°/sec. The dots had a limited lifetime of six frames (0.08 sec), upon completion of which each dot was randomly regenerated within the stimulus area. The form stimulus was a Glass pattern[33] generated by superimposing two identical copies of 250 random dots at the center of the display, with a linear displacement of 0.266° to create a translation Glass pattern. In essence, the dipoles in the Glass pattern are the spatial representation of two snapshots of the RDK stimulus captured in two different time frames. The direction of motion of the individual dot elements in the RDK and the orientation of the dipole elements in the Glass pattern were derived from a Gaussian distribution with a prescribed mean and SD that served as external noise (Fig. 1). The level of external noise was determined by the SD of the distribution with the mean of the distribution centered at different angles from the vertical reference (90°). The overall direction of the RDK and orientation of the Glass pattern (right or left of vertical) was randomized. For the strabismic amblyopes and remaining six normal controls (Experiment 2), both RDK and Glass patterns were composed of a total of 240 dots to facilitate the discrimination of Glass patterns (refer to discussion).

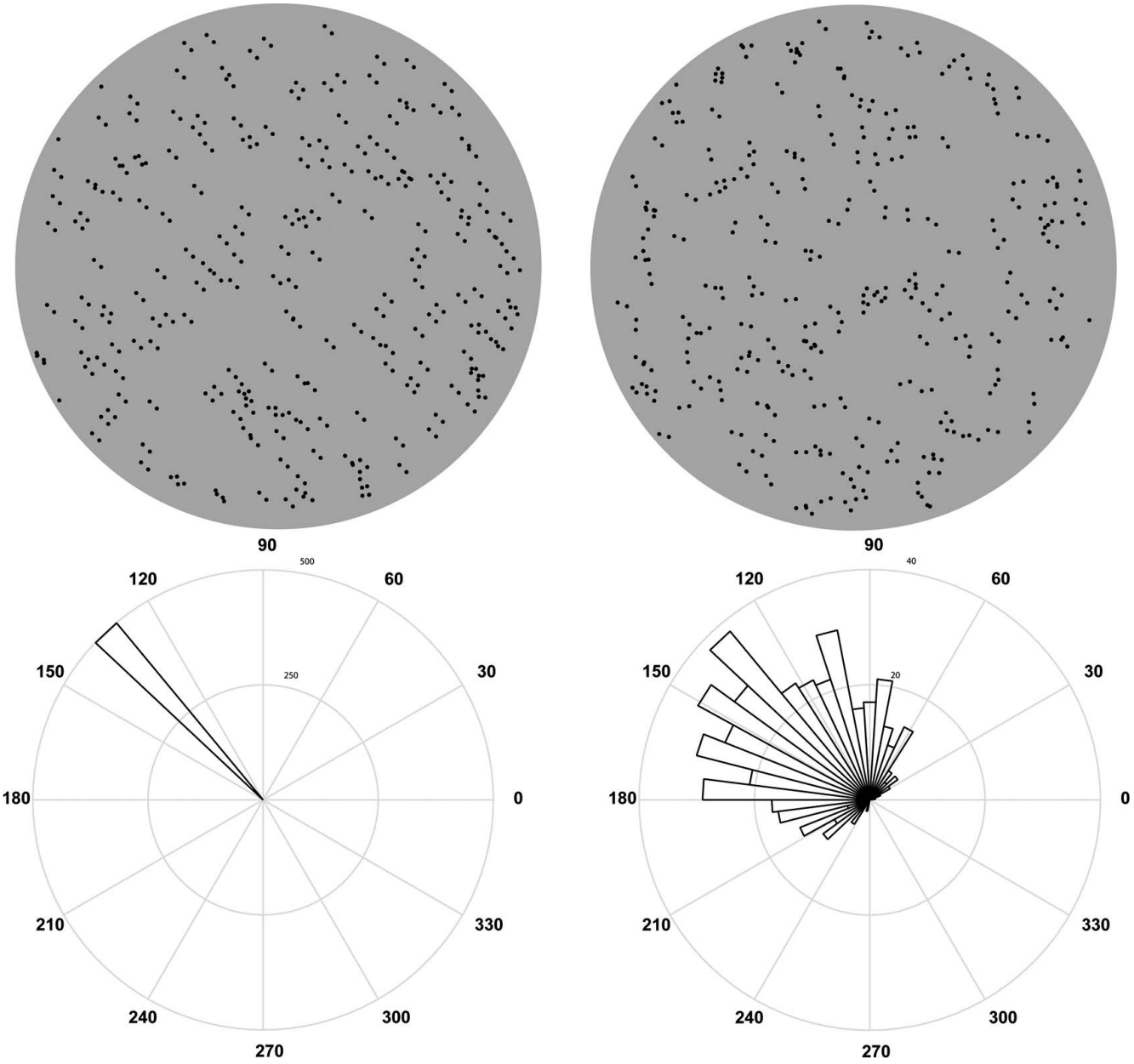

FIGURE 1. (*Top*) Example of Glass pattern stimuli with the same mean orientation and different variances. (*Bottom*) Angle histograms showing the distribution of dipole orientations in each pattern. The orientations of individual dipoles are generated from a Gaussian distribution with the mean (μ) of the distribution representing global orientation of the Glass pattern (*left of the vertical* shown here). The increase in the SD of the distribution (σ) increases the noise in the stimulus (*from left to right*).

Procedure

All participants completed the experiments in a dark room with the computer monitor being the only source of light. The participant's task in each trial was to discriminate the mean direction (RDK) of dots or orientation (Glass) of dipoles from the vertical (90°) reference.

To facilitate the data collection,[34] we first measured fine direction/orientation discrimination threshold at no noise where the overall direction/orientation in each trial was adaptively changed by the 3-down-1-up staircase. Then, the multiples (2× and 4× for anisometropic amblyopes and 3× only for strabismic amblyopes) of the initial direction/orientation thresholds at no noise were used to evaluate the threshold variance with a 3-down-1-up staircase. The staircase in no noise started with the mean direction/orientation of ±10° from vertical. The staircases in high noise condition started from a SD of 10° with the mean fixed at the multiples of direction/orientation threshold determined previously for each subject. All staircases terminated after 10 reversals or 100 trials, whichever was reached first. The thresholds were then calculated as a geometrical mean of the last seven reversals. All participants completed two sessions of 15 practice trials for each noise condition. Upon the satisfactory completion of the practice session, a full experimental session was commenced. The total time for each experiment (RDK or Glass pattern) including practice sessions was approximately 15 to 20 minutes.

The thresholds were modelled by the equation below to relate the direction/orientation offset thresholds to the external noise (σ_{ext}), internal equivalent noise (σ_{eq}) and

Table 2. The Table Provides the Mean Thresholds With the Values in Parenthesis Representing the Standard Deviation

	Glass		RDK	
Eyes	**No Noise**	**High Noise (y @ x)**	**No Noise**	**High Noise (y @ x)**
Normal	4.22 (2.19)	11.71 (1.73) @ 19.67 (1.77)	1.99 (1.72)	5.67 (1.50) @ 25.11 (1.45)
Aniso (Fellow)	4.36 (2.17)	14.19 (1.71) @ 16.83 (3.00)	2.55 (1.59)	5.63 (1.52) @19.79 (1.42)
Aniso (Amblyopic)	4.35 (1.98)	15.83 (1.66) @ 23.48 (1.43)	2.69 (1.23)	8.14 (1.50) @ 24.15 (1.66)
Strab (Fellow)	5.45 (1.76)	14.56 (1.62) @ 21.99 (1.14)	3.03 (1.52)	7.38 (1.71) @ 21.43 (1.24)
Strab (Amblyopic)	7.91 (1.34)	21.94 (1.23) @ 22.87 (1.39)	3.13 (1.70)	13.82 (1.45) @ 28.98 (1.35)

The data for the high noise condition represents the mean orientation/direction offset at (@) mean variance thresholds. Anisometropic, Ansio; Strabismic, Strab.

sampling efficiency (*Eff*) parameters.[35]

$$\tau_{obs} = \sqrt{\frac{\sigma_{eq}^2 + \sigma_{ext}^2}{Eff}} \quad (1)$$

For each task (Glass or RDK), the numbers of σ_{eq} & *Eff* needed to model the thresholds can range from two to six given the number of eyes (normal versus fellow versus amblyopic eye for patients). Among all the possible models, here we illustrate only four of them: a full model with six parameters (i.e., three pairs of σ_{eq} & *Eff* for normal, fellow and amblyopic eye); two models with four parameters (one σ_{eq} with three *Eff* or three σ_{eq} with one *Eff*); the most parsimonious model with two parameters (single σ_{eq} and *Eff*). Among the layers of nested models, the best model was selected by testing the goodness of fits between the models hierarchically with the following:

$$F(df_1, df_2) = \frac{(r_{full}^2 - r_{reduced}^2)/df_1}{(1 - r_{full}^2)/df_2} \quad (2)$$

Where, $df_1 = k_{full} - k_{reduced}$ and $df_2 = N - k_{full}$. The k is the number of parameters in each model, and N is the number of predicted data points.

Results

Figure 2 shows the raw thresholds for both Glass and RDK across the experiments 1 and 2. There was no significant difference in the orientation/direction discrimination thresholds for normal controls between experiments 1 and 2 using 500 and 240 dot stimuli ($PS > 0.05$). The thresholds for normal controls were hence collapsed for further data analysis. The thresholds for Glass were higher than RDK for all participants. The thresholds for the strabismic amblyopes were elevated compared to normal for both RDK and Glass. On the other hand, the thresholds for anisometropic amblyopes were similar to normal for both stimuli. Table 2 summarizes the Figure 2 by providing the mean thresholds at different noise levels for normal and amblyopes across tasks.

Experiment 1: Anisometropic Amblyopia

The nested models were statistically tested to determine the influence of internal noise/sampling efficiency on the orientation/direction discrimination. The nested model results for orientation discrimination are provided in Figure 3. All three reduced models (Figs. 3B–D) were similar to the full model (Fig. 3A), 1 σ_{eq} and 3 *Eff* [$F(2,62) = 0.163$, $P > 0.1$], 3 σ_{eq} with 1 *Eff* [$F(2,62) = 0.244$, $P > 0.1$], and 1 σ_{eq} with 1 *Eff* [$F(2,64) = 0.252$, $P > 0.1$]. Hence, the most parsimonious model (1 σ_{eq} and 1 *Eff*) showing no difference in parameters between normal, fellow, and amblyopic eyes was chosen as the best model.

Similar nested model analysis for the direction discrimination among normal, fellow, and amblyopic eyes showed that the simplest model with both σ_{eq} and *Eff* constrained across the eyes best described the threshold data [$F(2,64) = 2.84$, $P > 0.05$] (Fig. 4).

Experiment 2: Strabismic Amblyopia

All nine strabismic amblyopes completed the RDK experiment while only six could detect the Glass pattern structure. The

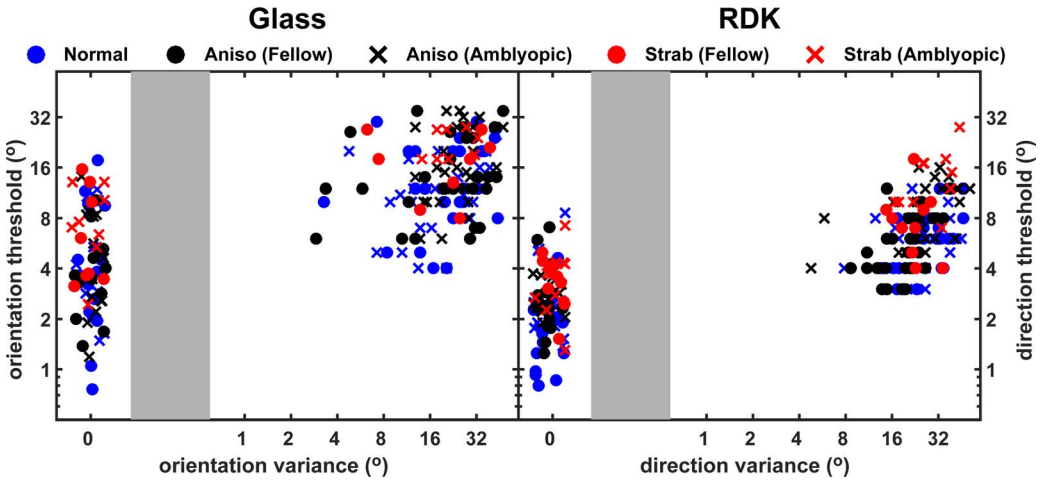

Figure 2. A scatterplot of individual thresholds for all participants for Glass and RDK. Small random jitters are added to the thresholds at no noise for better presentation.

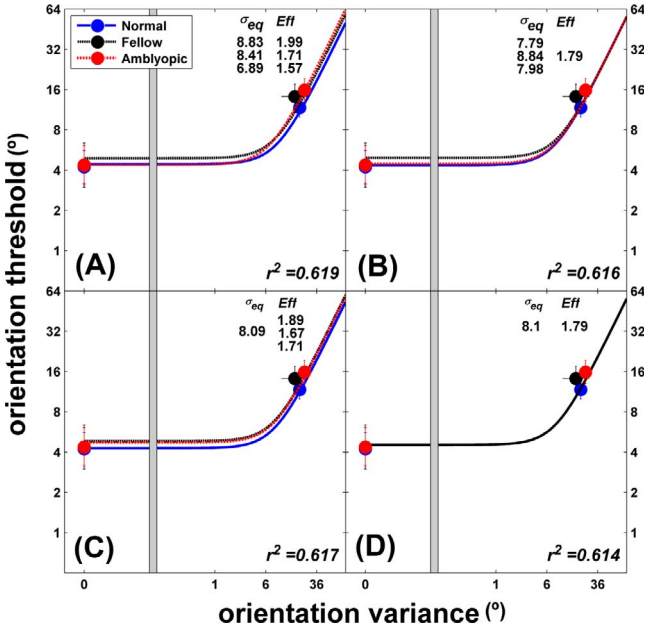

Figure 3. Nested models for the mean orientation discrimination data for the anisometropic amblyopes ($n = 8$) and normal controls ($n = 12$), relating the orientation offset and variance thresholds to different values of the internal noise and sampling efficiency; full model (**A**), reduced model with *Eff* constrained (**B**), reduced model with σ_{eq} constrained (**C**), and the simplest model with both σ_{eq} and *Eff* constrained (**D**). The best fitting parameters (σ_{eq} and *Eff*) and the goodness of fit (r^2) of each model are provided. *Error bars*: 95%CI. Two high noise conditions (2× and 4×) are averaged to represent a single high noise point.

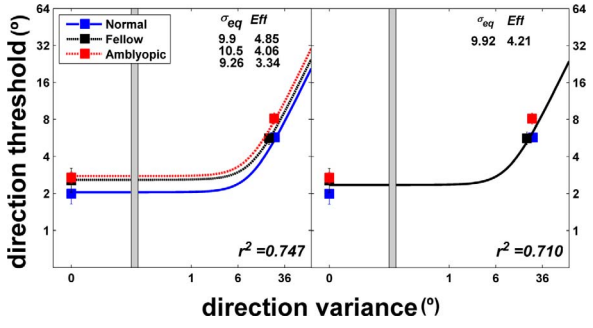

Figure 4. Nested models (*full, left panel and statistically chosen, right panel*) for the mean direction discrimination data for the anisometropic amblyopes ($n = 8$) and normal controls ($n = 12$), relating the direction offset and variance thresholds to different values of the internal noise and sampling efficiency. The best fitting parameters (σ_{eq} and *Eff*) and the goodness of fit (r^2) of each model are provided. *Error bars*: 95%CI.

Discussion

Global Motion Discrimination in Amblyopia

Fine global motion discrimination thresholds were normal in anisometropic amblyopia but abnormal in the strabismic amblyopes. This is in contrast to previous studies, which have reported normal thresholds in both types of amblyopia when using RDK composed of micro pattern elements.[15,18] These studies, however, initially normalized the local direction discrimination threshold (angle from vertical reference) of a single micro pattern element between the amblyopic and fellow eye by adjusting stimulus contrast then used the orientation and direction discrimination thresholds for the amblyopic eye were higher than both fellow eye and normal eye. The nested model testing (Fig. 5) showed that compared with the full model the reduced model with a single σ_{eq} and independent *Eff* was statistically the best model to describe the participants performance for both orientation discrimination [$F(2,22) = 0.42$, $P > 0.1$] and direction discrimination [$F(2,32) = 0.53$, $P > 0.1$]. The reduced models with σ_{eq} constrained for each domain were treated as the full model and further compared against the simplest model (1 σ_{eq} and 1 *Eff*). The results showed that the simplest model resulted in significantly poorer fits ($PS < 0.05$), confirming that the models with σ_{eq} constrained and independent *Eff* were the statistically the best models for both global orientation and direction discrimination.

The nested modelling showed that the difference in sampling efficiency best described the raised direction/orientation thresholds in strabismic amblyopes. To compare the individual strabismic sampling efficiency against the normal in each domain, the individual strabismic thresholds were fitted to the nested models with normal thresholds. The log sampling efficiency ratio of normal to amblyopic/fellow eye, respectively, (Fig. 6) was then calculated. The sampling efficiency was poorer in the amblyopic eye for both global motion and global form compared with the normal controls. The three amblyopes (SM, MR, and JR; Fig. 5A) who could not detect the Glass pattern structure also showed the poorest efficiency in the global motion task. For the fellow eye, seven of nine amblyopes had poorer efficiency for global motion and three out of six amblyopes showed poorer efficiency for the global form.

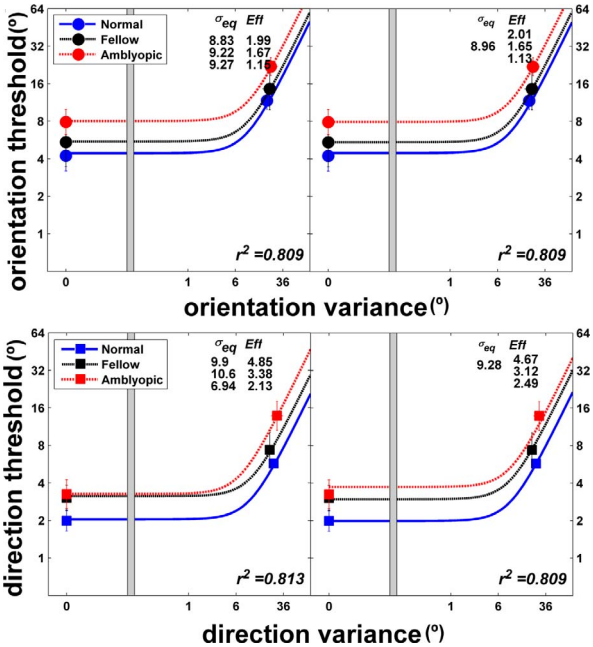

Figure 5. Nested models (*full, left panels and statistically chosen, right panels*) for the mean orientation discrimination threshold data for the normal ($n = 12$), fellow ($n = 6$), and amblyopic ($n = 6$) eyes (*upper panels*) and direction discrimination threshold data for the normal ($n = 12$), fellow ($n = 9$), and amblyopic ($n = 9$) eyes (*lower panels*). The orientation/direction offset and variance thresholds are related to different values of the internal noise and sampling efficiency. The best-fitting parameters (σ_{eq} and *Eff*) and the goodness of fit (r^2) of the each model is provided. *Error bars*: 95%CI.

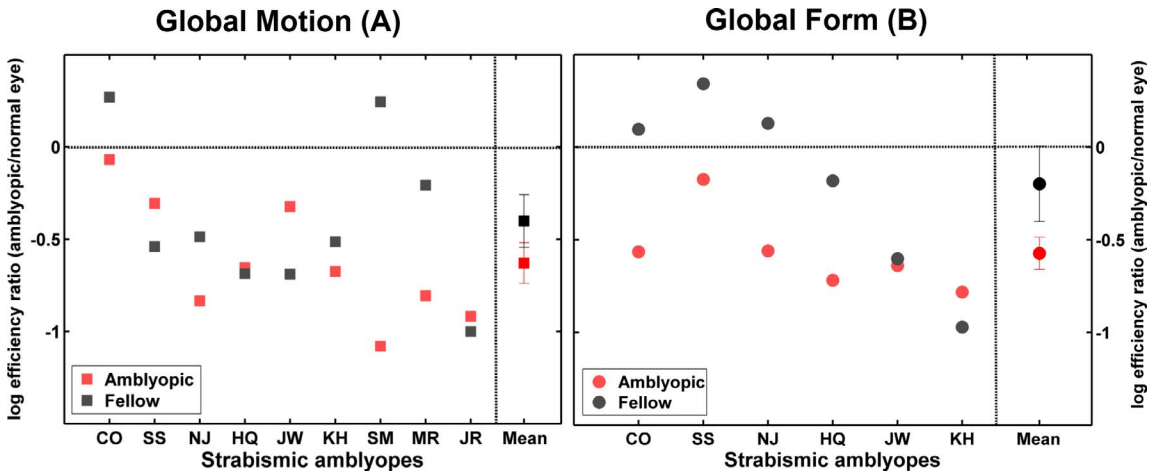

FIGURE 6. The log efficiency ratio (amblyopic/normal participant) for the global motion (**A**) and global form (**B**) for strabismic amblyopes and mean data. The data point lying above the *horizontal dotted lines* represents no deficiency in comparison to the normal eye; the points along the negative values represent how deficient the amblyopes are with respect to the normal. *Error bars*: 95%CI.

normalized contrast for the global motion discrimination with multiple micro patterns. In the current study, RDKs with high contrast dot elements (95%) were used to study both amblyopic and fellow eye performance. These differences in the stimulus and the experimental procedure may have resulted in different results obtained for strabismic amblyopia. Our results are, however, in line with previous reports of increased motion coherence thresholds in strabismic amblyopes.[13,14,16,17]

Differences in performance between anisometropic and strabismic amblyopia have been reported for a range of visual functions[36] such as optotype acuity,[37] vernier acuity,[38] and contrast sensitivity.[37] Such differences are supported by the results of physiological studies where a progressive reduction of neural responses in extra striate cortical areas has been reported in strabismic but not anisometropic[36] amblyopia.[39,40]

The nested model testing in this study revealed that the higher direction discrimination thresholds in strabismic amblyopes were due to a reduced efficiency at the global processing stage. The normal internal equivalent noise suggests that local motion processing is intact in both types of amblyopia, in agreement with other studies.[13,14,17,41] The direction sensitive cells stimulated by the amblyopic eye in V1 are also reported to be normal in anisometropic and strabismic primates.[40] Our finding of abnormal global processing in strabismic amblyopia is supported by previous physiological and imaging studies that reported a reduced contribution from the amblyopic eye to extra striate motion areas (MT, MST).[4,5] The results suggest that the local direction processing at early visual areas is normal in amblyopia with only the strabismic amblyopes showing a deficit at a later global processing stage.

Global Form Discrimination in Amblyopia

Global form perception in the Glass pattern was found to be normal in anisometropic amblyopia but abnormal in strabismic amblyopia. Notably, the strabismic amblyopes were not able to complete the evaluation for the Glass pattern with 500 dot elements used in the first experiment for anisometropic amblyopia. However, when the number of elements was reduced to 240, six of nine strabismic amblyopes could reliably detect the structure of the Glass pattern. This could have been due to the increase in correspondence noise in a Glass pattern with a higher dipole density. This dependency of performance in amblyopia on the number of elements has been previously reported for a mean orientation discrimination task with Gabor patches.[42] However, even with a reduced number of dipole elements, three strabismic amblyopes could still not reliably detect the Glass pattern structure.

As far as we are aware, this is the first study that used Glass pattern stimuli to determine fine orientation discrimination in amblyopia. Mansouri and Hess[15] reported normal thresholds in both anisometropic and strabismic amblyopes using Gabor patches in a global orientation discrimination task. However, other studies using similar Gabor patch stimuli have reported elevated orientation discrimination thresholds in both anisometropic and strabismic amblyopia.[11,21]

Our results are in agreement with studies that have used Glass patterns to report elevated global form coherence threshold in humans[19] and macaques[43] with amblyopia. Similarly the inability of some strabismic amblyopes to reliably detect the structure of the translational Glass pattern observed in the current study has also been reported previously.[19] This inability does not appear to be related to the severity of the amblyopia as an amblyope (MR) with the least IOD (0.26) and another amblyope (SM) with the largest IOD (0.6) failed to detect the Glass pattern. This is in line with previous report of inability of strabismic amblyope with relatively small IOD to detect the structure of translational Glass pattern.[19]

The apparent difference between these findings could be due to the differences in the processing of the different experimental stimuli (e.g., Gabor patches versus Glass pattern with dot elements). The orientation discrimination in a Glass pattern is based on extracting local orientation cues followed by the global averaging. However, in the line segment and Gabor patches the local orientation extraction does not seem necessary and the stimuli are processed as extended contours.[22] Hence, the discrimination of a Glass pattern is a more complex task than either the Gabor patches or the line segments. This possible difference is also reflected in better sensitivity to the line segments compared with the Glass pattern in visually normal participants.[44,45] Further the averaging in Gabor patches and line segments may be influenced by the local lateral connections in V1, and hence these stimuli are not recommended for the evaluation of a global orientation judgment.[22] Because lateral connections in V1 would be expected to have a minimal influence in the perception of a dipole Glass pattern our results are more likely to reflect true global orientation processing. Even with the relative ease of detection of line segment stimuli, a study

reported increased coherence thresholds for both the anisometropic and strabismic amblyopes with a translational line segment stimuli.[12]

The reduced fine orientation sensitivity in strabismic amblyopia appears to be due to the differences in the efficiency with which the local orientation cues are processed at the global level. The local orientation processing is also reported to be normal for simple grating stimuli[46] and Gabor patches,[47,48] once the spatial frequency and contrast deficiencies are accounted for. Simmers et al.[21] also reported normal local orientation discrimination abilities in both strabismic and anisometropic amblyopia with increased orientation coherence thresholds showing limited global processing.[21] Similarly physiological studies have also reported normal orientation selectivity in V1 cells isolated from anisometropic and strabismic amblyopic eyes.[40] The deficits in the global orientation processing meanwhile could be due to the reduced activity at the higher cortical areas of the ventral stream such as V4 and lateral occipital complex.[8]

Comparison of the Global Motion and Form Deficits in Amblyopia

The elevated thresholds for strabismic amblyopes along both domains were due to the under sampling of the local inputs at the global processing stage. This would suggest that the under sampling theory posited for other visual deficits in amblyopia[36,49] could be applicable to global motion and form processing as well. These deficits do not seem to be dependent on the visibility of stimuli as has been reported before for normal participants,[50] as the fellow eyes of strabismic amblyopes which had similar visual acuity to the normal eyes (independent *t*-test, $t\,(20) = 1.25$, $P > 0.05$) also showed raised thresholds for both motion and form domains.

Dorsal stream functions such as motion perception are reported to be affected in various developmental disorders including amblyopia,[12] leading to the suggestion of dorsal stream vulnerability.[22,23] Our results show that both streams are affected in strabismic amblyopia. However, some strabismic amblyopes were unable to even detect the structure of the Glass pattern, suggesting a more significant deficit for the perception of global form. The imaging and physiological studies also showed that both dorsal and ventral stream activity is reduced in amblyopia[4,5,7,8] while a study using amblyopic cats reported a larger deficit in the ventral stream compared to the dorsal stream.[39]

Two probable causes for a dorsal stream vulnerability are related to the anatomic aspects and the developmental trajectory of the dorsal stream.[23] The M-cells in retina and lateral geniculate nucleus, the early processors of the dorsal stream inputs, are more susceptible to the damage from pathologic changes due to their larger size and smaller population. In amblyopia, the deficits at the M-cell level should result in lower sensitivity at both local and global processing stages. But our results and a wide range of studies[13,14,17,41] suggest that the deficits in the motion domain are restricted mostly to the global processing level. Another explanation for the dorsal stream vulnerability in development disorders is due to the late development of the dorsal stream compared with the ventral stream functions.[23] For example, some studies reported that the global motion processing mechanisms follow a long and protracted developmental pattern extending beyond 14 years.[51–53] However, there are other studies reporting a similar maturation age for both global form and motion processing.[54,55]

Recent studies question the generalizability of dorsal stream vulnerability in neurologic developmental disorders.[22] For example, it is argued that most studies that reported dorsal stream vulnerability used incompatible stimuli to allow for a direct comparison between the visual processing streams.[22] Additionally, the global processing deficits in motion and form processing in developmental disorders including amblyopia seem to be task and stimuli dependent, hence generalizing the results from one task or stimuli as dorsal or ventral stream vulnerability may not be accurate.

Our results using similar random dot stimuli across the motion and form processing pathways suggest that tasks attributed to both the dorsal and ventral streams are affected in strabismic amblyopia with normal thresholds in anisometropic amblyopia. The results seem to suggest that the processing deficit in strabismic amblyopes is specific to the global processing stage along the higher extra striate areas ruling out the direct influence of the lower level deficits. In addition, the inability of some amblyopes to simply detect the structure formed by the Glass pattern would suggest a more profound deficit pertaining to ventral stream processing. This is contrary to the dorsal stream vulnerability previously reported in amblyopia, highlighting the need for further investigation.

Acknowledgements

Supported by the Visual Research Trust Equipment Grant R4304 (Glasgow, UK).

Disclosure: **M.R. Joshi**, None; **A.J. Simmers**, None; **S.T. Jeon**, None

References

1. Hess RF. Amblyopia: site unseen. *Clin Exp Opt*. 2001;84:321–336.
2. Wiesel TN, Hubel DH. Extent of recovery from the effects of visual deprivation in kittens. *J Neurophysiol*.1965;28:1060–1072.
3. Wiesel TN, Hubel DH. Single-Cell response in striate cortex of kittens deprived of vision in one eye. *J Neurophysiol*.1963;26:1003–1017.
4. El-Shamayleh Y, Kiorpes L, Kohn A, Movshon JA. Visual motion processing by neurons in area MT of macaque monkeys with experimental amblyopia. *J Neurosci*. 2010;30:12198–12209.
5. Thompson B, Villeneuve MY, Casanova C, Hess RF. Abnormal cortical processing of pattern motion in amblyopia: evidence from fMRI. *NeuroImage*. 2012;60:1307–1315.
6. Movshon JA, Eggers HM, Gizzi MS, Hendrickson AE, Kiorpes L, Boothe RG. Effects of early unilateral blur on the macaque's visual system. III. Physiological observations. *J Neurosci*. 1987;7:1340–1351.
7. Lerner Y, Pianka P, Azmon B, et al. Area-specific amblyopic effects in human occipitotemporal object representations. *Neuron*. 2003;40:1023–1029.
8. Muckli L, Kieß S, Tonhausen N, Singer W, Goebel R, Sireteanu R. Cerebral correlates of impaired grating perception in individual, psychophysically assessed human amblyopes. *Vision Res*. 2006;46:506–526.
9. Morrone MC, Burr DC, Vaina LM. Two stages of visual processing for radial and circular motion. *Nature*. 1995;376:507–509.
10. Wilkinson F, Wilson HR. Detection of global structure in Glass patterns: implications for form vision. *Vision Res*. 1998;38:2933–2947.
11. Husk JS, Hess RF. Global processing of orientation in amblyopia. *Vision Res*. 2013;82:22–30.
12. Simmers AJ, Ledgeway T, Hess RF. The influences of visibility and anomalous integration processes on the perception of global spatial form versus motion in human amblyopia. *Vision Res*. 2005;45:449–460.

13. Simmers AJ, Ledgeway T, Hess RF, McGraw PV. Deficits to global motion processing in human amblyopia. *Vision Res*. 2003;43:729–738.
14. Simmers AJ, Ledgeway T, Mansouri B, Hutchinson CV, Hess RF. The extent of the dorsal extra-striate deficit in amblyopia. *Vision Res*. 2006;46:2571–2580.
15. Mansouri B, Hess RF. The global processing deficit in amblyopia involves noise segregation. *Vision Res*. 2006;46: 4104–4117.
16. Aaen-Stockdale C, Ledgeway T, Hess RF. Second-order optic flow deficits in amblyopia. *Invest Ophthalmol Vis Sci*. 2007; 48:5532–5538.
17. Aaen-Stockdale C, Hess RF. The amblyopic deficit for global motion is spatial scale invariant. *Vision Res*. 2008;48:1965–1971.
18. Hess RF, Mansouri B, Dakin SC, Allen HA. Integration of local motion is normal in amblyopia. *J Opt Soc Am A*. 2006;23:986–992.
19. Rislove EM, Hall EC, Stavros KA, Kiorpes L. Scale-dependent loss of global form perception in strabismic amblyopia. *J Vis*. 2010;10(12):25.
20. Dallala R, Wang Y-Z, Hess RF. The global shape detection deficit in strabismic amblyopia: Contribution of local orientation and position. *Vision Res*. 2010;50:1612–1617.
21. Simmers AJ, Bex PJ. The representation of global spatial structure in amblyopia. *Vision Res*. 2004;44:523–533.
22. Grinter EJ, Maybery MT, Badcock DR. Vision in developmental disorders: is there a dorsal stream deficit? *Brain Res Bull*. 2010;82:147–160.
23. Braddick O, Atkinson J, Wattam-Bell J. Normal and anomalous development of visual motion processing: motion coherence and 'dorsal-stream vulnerability'. *Neuropsychologia*. 2003;41: 1769–1784.
24. Hamm LM, Black J, Dai S, Thompson B. Global processing in amblyopia: a review. *Front Psychol*. 2014;5:583.
25. Milner AD, Goodale MA. Two visual systems re-viewed. *Neuropsychologia*. 2008;46:774–785.
26. Livingstone M, Hubel D. Psychophysical evidence for separate channels for the perception of form, color, movement, and depth. *J Neurosci*. 1987;7:3416–3468.
27. Braddick OJ, O'Brien JMD, Rees G, Wattam-Bell J, Atkinson J, Turner R. Quantitative neural responses to form coherence in human extrastriate cortex. Paper presentend at: Neuroscience 2002. Washington, DC, November 7, 2002. Society for Neuroscience 32nd Annual Meeting.
28. Braddick OJ, O'Brien JM, Wattam-Bell J, Atkinson J, Hartley T, Turner R. Brain areas sensitive to coherent visual motion. *Perception*. 2001;30:61–72.
29. Simmers AJ, Ledgeway T, Hess RF, McGraw PV. Deficits to global motion processing in human amblyopia. *Vision Res*. 2003;43:729–738.
30. Dakin SC, Mareschal I, Bex PJ. Local and global limitations on direction integration assessed using equivalent noise analysis. *Vision Res*. 2005;45:3027–3049.
31. Brainard DH. The Psychophysics Toolbox. *Spat Vis*. 1997;10: 433–436.
32. Pelli DG. The VideoToolbox software for visual psychophysics: transforming numbers into movies. *Spat Vis*. 1997;10:437–442.
33. Glass L. Moire effect from random dots. *Nature*. 1969;223: 578–580.
34. Tibber MS, Kelly MG, Jansari A, Dakin SC, Shepherd AJ. An inability to exclude visual noise in migraine. *Invest Ophthalmol Vis Sci*. 2014;55:2539–2546.
35. Pelli DG. Effects of Visual Noise. Cambridge: Cambridge University; 1981.
36. Kiorpes L, McKee SP. Neural mechanisms underlying amblyopia. *Curr Opin Neurobiol*. 1999;9:480–486.
37. Levi DM, McKee SP, Movshon JA. Visual deficits in anisometropia. *Vision Res*. 2011;51:48–57.
38. Levi DM, Klein SA. Vernier acuity, crowding and amblyopia. *Vision Res*. 1985;25:979–991.
39. Schröder J-H, Fries P, Roelfsema PR, Singer W, Engel AK. Ocular dominance in extrastriate cortex of strabismic amblyopic cats. *Vision Res*. 2002;42:29–39.
40. Kiorpes L, Kiper DC, O'Keefe LP, Cavanaugh JR, Movshon JA. Neuronal correlates of amblyopia in the visual cortex of Macaque monkeys with experimental strabismus and anisometropia. *J Neurosci*. 1998;18:6411–6424.
41. Thompson B, Richard A, Churan J, Hess RF, Aaen-Stockdale C, Pack CC. Impaired spatial and binocular summation for motion direction discrimination in strabismic amblyopia. *Vision Res*. 2011;51:577–584.
42. Mansouri B, Allen HA, Hess RF, Dakin SC, Ehrt O. Integration of orientation information in amblyopia. *Vision Res*. 2004;44: 2955–2969.
43. Kiorpes L. Visual processing in amblyopia: animal studies. *Strabismus*. 2006;14:3–10.
44. Aspell JE, Wattam-Bell J, Braddick O. Interaction of spatial and temporal integration in global form processing. *Vision Res*. 2006;46:2834–2841.
45. Dakin SC. The detection of structure in glass patterns: psychophysics and computational models. *Vision Res*. 1997; 37:2227–2246.
46. Skottun BC, Bradley A, Freeman RD. Orientation discrimination in amblyopia. *Invest Ophthalmol Vis Sci*. 1986;27:532–537.
47. Demanins R, Hess RF, Williams CB, Keeble DRT. The orientation discrimination deficit in strabismic amblyopia depends upon stimulus bandwidth. *Vision Res*. 1999;39: 4018–4031.
48. Hess RF, Malin SA. Threshold vision in amblyopia: orientation and phase. *Invest Ophthalmol Vis Sci*. 2003;44:4762–4771.
49. Wang H, Levi DM, Klein SA. Spatial uncertainty and sampling efficiency in amblyopic position acuity. *Vision Res*. 1998;38: 1239–1251.
50. Burton EA, Wattam-Bell J, Rubin GS, Atkinson J, Braddick O, Nardini M. The effect of blur on cortical responses to global form and motion. *J Vis*. 2015;15(15):12.
51. Gunn A, Cory E, Atkinson J, et al. Dorsal and ventral stream sensitivity in normal development and hemiplegia. *Neuroreport*. 2002;13:843–847.
52. Hadad BS, Maurer D, Lewis TL. Long trajectory for the development of sensitivity to global and biological motion. *Dev Sci*. 2011;14:1330–1339.
53. Joshi MR, Falkenberg HK. Development of radial optic flow pattern sensitivity at different speeds. *Vision Res*. 2015; 110(part A):68–75.
54. Gordon G, McCulloch D. A VEP investigation of parallel visual pathway development in primary school age children. *Doc Ophthalmol*. 1999;99:1–10.
55. Parrish EE, Giaschi DE, Boden C, Dougherty R. The maturation of form and motion perception in school age children. *Vision Res*. 2005;45:827–837.

Investigative Ophthalmology & Visual Science